Coulomb-corrected eikonal description of the breakup of halo nuclei

P. Capel,[1,*] D. Baye,[1,†] and Y. Suzuki[2,‡]
[1]*Physique Quantique, C.P. 165/82 and Physique Nucléaire Théorique et Physique Mathématique, C.P. 229 Université Libre de Bruxelles, B 1050 Brussels, Belgium*
[2]*Department of Physics, Niigata University, Niigata 950-2181, Japan*
(Received 23 May 2008; published 7 November 2008)

The eikonal description of breakup reactions diverges because of the Coulomb interaction between the projectile and the target. This divergence is due to the adiabatic, or sudden, approximation usually made, which is incompatible with the infinite range of the Coulomb interaction. A correction for this divergence is analyzed by comparison with the dynamical eikonal approximation, which is derived without the adiabatic approximation. The correction consists in replacing the first-order term of the eikonal Coulomb phase by the first-order of the perturbation theory. This allows taking into account both nuclear and Coulomb interactions on the same footing within the computationally efficient eikonal model. Excellent results are found for the dissociation of ^{11}Be on lead at 69 MeV/nucleon. This Coulomb-corrected eikonal approximation provides a competitive alternative to more elaborate reaction models for investigating breakup of three-body projectiles at intermediate and high energies.

DOI: 10.1103/PhysRevC.78.054602 PACS number(s): 24.10.−i, 25.60.Gc, 03.65.Nk, 27.20.+n

I. INTRODUCTION

Halo nuclei are among the most peculiar quantum structures [1–3]. These light neutron-rich nuclei exhibit a very large matter radius when compared to their isobars. This extended matter distribution is due to the weak binding of one or two valence neutrons. Thanks to their low separation energy, these neutrons tunnel far inside the classically forbidden region and have a high probability of presence at a large distance from the other nucleons. In a simple point of view, they can be seen as very clusterized systems: a core that contains most of the nucleons, and that resembles a usual nucleus, to which one or two neutrons are loosely bound and form a sort of halo around the core [4]. The ^{11}Be, ^{15}C, and ^{19}C isotopes are examples of one-neutron halo nuclei. Examples of two-neutron halo nuclei are ^{6}He, ^{11}Li, and ^{14}Be. In addition to their two-neutron halo, these nuclei also exhibit the Borromean property [5]: the three-body system is bound although none of the two-body subsystem is.

Since their discovery in the mid-1980s [6], these nuclei have thus been the focus of many experimental [1–3] and theoretical [7–9] studies. Due to their short lifetime, halo nuclei cannot be studied with usual spectroscopic techniques, and one must resort to indirect methods to infer information about their structure. Breakup reactions are among the most used methods to study halo nuclei [10–12]. In such reactions, the halo dissociates from the core through interaction with a target. To extract valuable information from experimental data one needs an accurate reaction model coupled to a realistic description of the projectile. Various techniques have been developed with this aim: perturbation expansion [13,14], adiabatic approximation [15], eikonal model [16–18], coupled-channels with a discretized continuum (CDCC) [19–21], numerical resolution of a three-dimensional time-dependent Schrödinger equation (TDSE) [22–27], and, more recently, dynamical eikonal approximation (DEA) [28–30].

Some of these techniques (perturbation expansion, adiabatic approximation, and the eikonal model) are based on approximations that lead to easy-to-handle models. Their main advantage is their relative simplicity in use and interpretation. However, the approximations on which they are built usually restrain their validity domain. For example, perturbative and adiabatic models are restricted to the sole Coulomb interaction between the projectile and the target. The eikonal method on the contrary diverges for that interaction and can be used only for reactions on light targets. The adiabatic, or sudden, approximation made in the usual eikonal model is responsible for that divergence. It indeed assumes a very brief collision time that is incompatible with the infinite range of the Coulomb interaction.

The more elaborate models (CDCC, TDSE, and DEA) are not restricted in the choice of the projectile-target interaction. However, they lead to complex and time-consuming implementations. First calculations were therefore limited to simple descriptions of the projectile (i.e., two-body projectiles with local core-halo interactions). Recently, several attempts have been made to improve the description of the projectile. For example, Summers, Nunes, and Thompson have developed an extended version of the CDCC technique, baptized XCDCC, in which the description of the halo nucleus includes excitation of the core [31]. Other groups are developing four-body CDCC codes, i.e., a description of the breakup of three-body projectiles, with the aim of modeling the dissociation of Borromean nuclei [32,33]. These techniques, albeit promising, require large computational facilities and are very time-consuming.

Alternatively, one could try to extend the range of simpler descriptions of breakup reactions. Among these descriptions, the eikonal model is of particular interest. It indeed allows taking into account, at all orders and on the same footing, both nuclear and Coulomb interactions between the projectile and the target. Moreover, it gives excellent results for

*pierre.capel@centraliens.net
†dbaye@ulb.ac.be
‡suzuki@nt.sc.niigata-u.ac.jp

nuclear-dominated dissociations [17,29]. Its only flaw is the erroneous treatment of the Coulomb interaction. A correction to that treatment has been proposed by Margueron, Bonaccorso, and Brink [34] and developed by Abu-Ibrahim and Suzuki [35]. The basic idea of this Coulomb-corrected eikonal model (CCE) is to replace the diverging Coulomb eikonal phase at first-order by the corresponding first-order of the perturbation theory [36]. The latter, being obtained without adiabatic approximation, does not diverge. The CCE is much more economical than more elaborate techniques (a gain of a factor 100 in computational time can be achieved between this CCE and the DEA). It could therefore constitute a competitive alternative for simulating the breakup of Borromean nuclei at intermediate and high energies. However efficient it seems, this correction has never been compared to any other reaction model.

In this work, we aim at evaluating the validity and analyzing the strengths and weaknesses of this correction by comparing it with the DEA. The chosen test cases are the breakup of ^{11}Be on Pb and C so as to see the significance of the correction for both heavy and light targets. The considered energy is around 70 MeV/nucleon. This corresponds to RIKEN experiments [11,12], with which the DEA is in excellent agreement [28,29].

Our article is organized as follows. In Sec. II, we recall the basics of the eikonal description of reactions and detail the Coulomb correction proposed in Refs. [34,35]. The numerical aspects of our calculations are summarized in Sec. III. The results for ^{11}Be on Pb are detailed in Sec. IV, whereas those corresponding to a carbon target are given in Sec. V. The final section contains our conclusions about this model.

II. THEORETICAL FRAMEWORK

A. Eikonal description of breakup reactions

To describe the breakup of a halo nucleus, we consider the following three-body model. The projectile P is made up of a fragment f of mass m_f and charge $Z_f e$, initially bound to a core c of mass m_c and charge $Z_c e$. This two-body projectile is impinging on a target T of mass m_T and charge $Z_T e$. The fragment has spin I, whereas both core and target are assumed to be of spin zero. These three bodies are seen as structureless particles.

The structure of the projectile is described by the internal Hamiltonian

$$H_0 = \frac{p^2}{2\mu_{cf}} + V_{cf}(\boldsymbol{r}), \tag{1}$$

where $\boldsymbol{r}$ is the relative coordinate of the fragment to the core, $\boldsymbol{p}$ is the corresponding momentum, $\mu_{cf} = m_c m_f/m_P$ is the reduced mass of the core-fragment pair (with $m_P = m_c + m_f$), and V_{cf} is the potential describing the core-fragment interaction. This potential includes a central part and a spin-orbit coupling term (see Sec. III).

In partial wave lj, the eigenstates of H_0 are defined by

$$H_0\phi_{ljm}(E,\boldsymbol{r}) = E\phi_{ljm}(E,\boldsymbol{r}), \tag{2}$$

where E is the energy of the c-f relative motion and j is the total angular momentum resulting from the coupling of the orbital momentum l with the fragment spin I. The negative-energy solutions of Eq. (2) correspond to the bound states of the projectile. They are normed to unity. The positive-energy states describe the broken-up projectile. Their radial part u_{klj} are normalized according to

$$u_{klj}(r) \underset{r\to\infty}{\longrightarrow} \cos\delta_{lj} F_l(kr) + \sin\delta_{lj} G_l(kr), \tag{3}$$

where $k = \sqrt{2\mu_{cf}E/\hbar^2}$ is the wave number, δ_{lj} is the phase shift at energy E, and F_l and G_l are, respectively, the regular and irregular Coulomb functions [37].

The interactions between the projectile constituents and the target are simulated by optical potentials chosen in the literature (see Sec. III). Within this framework the description of the reaction reduces to the resolution of a three-body Schrödinger equation that reads, in the Jacobi set of coordinates illustrated in Fig. 1,

$$\left[\frac{P^2}{2\mu} + H_0 + V_{PT}(\boldsymbol{R},\boldsymbol{r})\right]\Psi(\boldsymbol{R},\boldsymbol{r}) = E_T\Psi(\boldsymbol{R},\boldsymbol{r}), \tag{4}$$

where $\boldsymbol{R}$ is the coordinate of the projectile center of mass relative to the target, $\boldsymbol{P}$ is the corresponding momentum, $\mu = m_P m_T/(m_P + m_T)$ is the projectile-target reduced mass, and E_T is the total energy. The projectile-target interaction

$$V_{PT}(\boldsymbol{R},\boldsymbol{r}) = V_{cT}\left(\boldsymbol{R} - \frac{m_f}{m_P}\boldsymbol{r}\right) + V_{fT}\left(\boldsymbol{R} + \frac{m_c}{m_P}\boldsymbol{r}\right), \tag{5}$$

is the sum of the optical potentials V_{cT} and V_{fT} (including Coulomb) that simulate the core-target and fragment-target interactions, respectively. The projectile impinging on the target is initially bound in the state $\phi_{l_0 j_0 m_0}$ of energy E_0. We are therefore interested in solutions of Eq. (4) that behave asymptotically as

$$\Psi(\boldsymbol{R},\boldsymbol{r}) \underset{Z\to-\infty}{\longrightarrow} e^{i\{KZ+\eta\ln[K(R-Z)]\}}\phi_{l_0 j_0 m_0}(E_0,\boldsymbol{r}), \tag{6}$$

where Z is the component of $\boldsymbol{R}$ in the incident-beam direction and $\eta = Z_T Z_P e^2/(4\pi\epsilon_0\hbar v)$ is the P-T Sommerfeld parameter (with $Z_P = Z_c + Z_f$).

In the eikonal description of reactions, the three-body wave function Ψ is factorized as the product of a plane wave by a new function $\widehat{\Psi}$ [16–18],

$$\Psi(\boldsymbol{R},\boldsymbol{r}) = e^{iKZ}\widehat{\Psi}(\boldsymbol{R},\boldsymbol{r}), \tag{7}$$

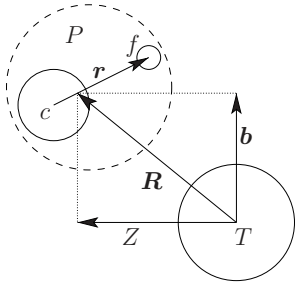

FIG. 1. Jacobi set of coordinates: $\boldsymbol{r}$ is the projectile internal coordinate, and $\boldsymbol{R} = \boldsymbol{b} + Z\widehat{\boldsymbol{Z}}$ is the target-projectile coordinate.

where K is the wave number of the projectile-target relative motion related to the total energy E_T by

$$E_T = \frac{\hbar^2 K^2}{2\mu} + E_0. \tag{8}$$

With factorization (7), the Schrödinger equation (4) reads

$$\left[\frac{P^2}{2\mu} + vP_Z + H_0 - E_0 + V_{PT}(\boldsymbol{R}, \boldsymbol{r})\right] \widehat{\Psi}(\boldsymbol{R}, \boldsymbol{r}) = 0, \tag{9}$$

where $v = \hbar K/\mu$ is the initial projectile-target relative velocity. The first step in the eikonal approximation is to assume the second-order derivative $P^2/2\mu$ negligible with respect to the first-order derivative vP_Z. The function $\widehat{\Psi}$ is indeed expected to vary weakly in $\boldsymbol{R}$ when the collision occurs at sufficiently high energy [16–18]. This leads to the DEA Schrödinger equation [28,29]

$$i\hbar v \frac{\partial}{\partial Z} \widehat{\Psi}(\boldsymbol{b}, Z, \boldsymbol{r}) = [(H_0 - E_0) + V_{PT}(\boldsymbol{R}, \boldsymbol{r})] \widehat{\Psi}(\boldsymbol{b}, Z, \boldsymbol{r}), \tag{10}$$

where the dependence of the wave function on the longitudinal Z and transverse $\boldsymbol{b}$ parts of the projectile-target coordinate $\boldsymbol{R}$ has been made explicit (see Fig. 1). This equation is mathematically equivalent to a time-dependent Schrödinger equation with straight-line trajectories and can be solved using any algorithm valid for the time-dependent Schrödinger equation (see, e.g., Refs. [22–27]). However, contrary to time-dependent models, it is obtained without semiclassical approximation: the projectile-target coordinate components $\boldsymbol{b}$ and Z are quantal variables in DEA. This advantage over time-dependent techniques allows taking into account interferences between solutions obtained at different bs. The DEA reproduces various breakup observables quite accurately for collisions of loosely bound projectiles on both light and heavy targets [29,30].

The second step in the usual eikonal model is to assume the collision to occur during a very brief time and to consider the internal coordinates of the projectile to be frozen while the reaction takes place [17]. This second assumption, known as the adiabatic, or sudden, approximation leads to neglecting the term $H_0 - E_0$ in Eq. (10) that then reads

$$i\hbar v \frac{\partial}{\partial Z} \widehat{\Psi}(\boldsymbol{b}, Z, \boldsymbol{r}) = V_{PT}(\boldsymbol{R}, \boldsymbol{r}) \widehat{\Psi}(\boldsymbol{b}, Z, \boldsymbol{r}). \tag{11}$$

In these notations, the asymptotic condition (6) becomes

$$\widehat{\Psi}(\boldsymbol{b}, Z, \boldsymbol{r}) \underset{Z \to -\infty}{\longrightarrow} e^{i\eta \ln[K(R-Z)]} \phi_{l_0 j_0 m_0}(E_0, \boldsymbol{r}). \tag{12}$$

The solution of Eq. (11) exhibits the well-known eikonal expression [16]

$$\widehat{\Psi}(\boldsymbol{b}, Z, \boldsymbol{r}) = \exp\left[-\frac{i}{\hbar v} \int_{-\infty}^{Z} V_{PT}(\boldsymbol{b}, Z', \boldsymbol{r}) dZ'\right] \phi_{l_0 j_0 m_0}(E_0, \boldsymbol{r}). \tag{13}$$

This expression is valid only for short-range potentials. The Coulomb interaction requires a special treatment that is detailed in the next section. Let us point out that this treatment allows taking properly account of the projectile-target Rutherford scattering. The Coulomb distortion in Eq. (12) is therefore simulated in the phase of Eq. (13). After the collision, the whole information about the change in the projectile wave function is thus contained in the phase shift χ that reads

$$\chi(\boldsymbol{b}, \boldsymbol{s}) = -\frac{1}{\hbar v} \int_{-\infty}^{\infty} V_{PT}(\boldsymbol{R}, \boldsymbol{r}) dZ. \tag{14}$$

Due to translation invariance, this eikonal phase depends only on the transverse components $\boldsymbol{b}$ of the projectile-target coordinate $\boldsymbol{R}$ and $\boldsymbol{s}$ of the core-fragment coordinate $\boldsymbol{r}$.

B. Coulomb correction to the eikonal model

The eikonal model gives excellent results for nuclear-dominated reactions [17,29]. However, it suffers from two divergence problems when the Coulomb interaction becomes significant. The first is the well-known logarithmic divergence of the eikonal phase describing the Coulomb elastic scattering [16–18]. The second is caused by the adiabatic approximation used in the eikonal treatment of the Coulomb breakup [17]. To explain this, let us divide the eikonal phase (14) into its nuclear and Coulomb contributions

$$\chi(\boldsymbol{b}, \boldsymbol{s}) = \chi^N(\boldsymbol{b}, \boldsymbol{s}) + \chi^C(\boldsymbol{b}, \boldsymbol{s}) + \chi^C_{PT}(b). \tag{15}$$

The Coulomb term χ^C for a one-neutron halo nucleus reads (the extension to the case of a charged fragment is immediate) [29,35]

$$\chi^C(\boldsymbol{b}, \boldsymbol{s}) = -\eta \int_{-\infty}^{\infty} \left(\frac{1}{\left|\boldsymbol{R} - \frac{m_f}{m_P}\boldsymbol{r}\right|} - \frac{1}{R}\right) dZ \tag{16}$$

$$= \eta \ln\left(1 - 2\frac{m_f}{m_P}\frac{\widehat{\boldsymbol{b}} \cdot \boldsymbol{s}}{b} + \frac{m_f^2}{m_P^2}\frac{s^2}{b^2}\right), \tag{17}$$

$\widehat{\boldsymbol{b}}$ denotes a unit vector along the transverse coordinate $\boldsymbol{b}$. In Eq. (16), we subtract the term $1/R$ corresponding to a Coulomb interaction between the projectile center-of-mass and the target. The phase χ^C therefore corresponds to the Coulomb tidal force that contributes to the breakup. Moreover, this subtraction leads to a faster decrease of the potential at large distances, which enables us to obtain the analytic expression (17). This is compensated by the addition of the elastic Coulomb phase χ^C_{PT}

$$\chi^C_{PT}(b) = -\eta \int_{-Z_{\max}}^{Z_{\max}} \frac{dZ}{R}. \tag{18}$$

This phase describes the Rutherford scattering between the projectile and the target. The integral is truncated, for it otherwise diverges (note that the integral in Eq. (17) does not diverge and therefore does not require the same treatment). This truncation basically corresponds to Glauber's screened Coulomb potential [16]. Other truncation techniques [16] and other ways to deal with this divergence [18] exist. All lead to the same expression of the elastic Coulomb phase but for an additional constant phase that does not affect the cross sections [16]. The truncation considered in Eq. (18) leads to

$$\chi^C_{PT}(b) \approx 2\eta \ln \frac{b}{2Z_{\max}}. \tag{19}$$

This elastic Coulomb phase correctly reproduces Rutherford scattering, indicating that the first of the two aforementioned divergences can be easily corrected [16–18]. The nuclear term χ^N is then by definition the difference between the eikonal phase (14) and the Coulomb contributions (17) and (19).

In addition to the divergence in elastic scattering, the Coulomb interaction is responsible for a divergence in breakup. The aim of the present article is to analyze a way to correct this divergence. It is due to the slow decrease of χ^C in b. Indeed, when expanded in powers of χ^C, the exponential of the Coulomb eikonal phase reads

$$e^{i\chi^C} = 1 + i\chi^C - \tfrac{1}{2}(\chi^C)^2 + \cdots, \tag{20}$$

where the explicit dependence on the coordinates has been omitted for clarity. When integrated over b in the calculation of the cross sections (see Sec. II C), the $1/b$ asymptotic behavior of the first-order term $i\chi^C$ will lead to divergence.

This divergence problem arises from the incompatibility between the infinite range of the Coulomb interaction and the adiabatic, or sudden, approximation: no short collision time can be assumed if the Coulomb interaction dominates. Renouncing the use of the adiabatic approximation solves this divergence: the DEA, which corresponds to the eikonal model without this approximation {see Eq. (10) and Refs. [28,29]}, does not diverge. The excellent results obtained within the DEA for collisions of loosely bound projectiles on both light and heavy targets [29,30] confirm that, when dynamical effects are considered, both nuclear and Coulomb interactions can be properly taken into account on the same footing.

To avoid this divergence, a cutoff at large b could be made. In Ref. [38], Abu-Ibrahim and Suzuki proposed to limit the values of b to be considered in the cross-section calculations at

$$b_{\max} = \frac{\hbar v}{2|E_0|}. \tag{21}$$

This cutoff is obtained by requiring the characteristic time of internal excitation $\hbar/|E_0|$ to be shorter than the collision time b/v. The factor of 2 is proposed as a qualitative guide. However, this treatment is rather artificial and not very satisfactory [35].

Alternatively, it has been proposed by Margueron, Bonaccorso, and Brink [34], and developed by Abu-Ibrahim and Suzuki [35], to replace the first-order term $i\chi^C$ in Eq. (20), which leads to the divergence, by the first-order term of the perturbation theory $i\chi^{\mathrm{FO}}$ [36]

$$\chi^{\mathrm{FO}}(\boldsymbol{b},\boldsymbol{r}) = -\eta\int_{-\infty}^{\infty} e^{i\omega Z/v}\left(\frac{1}{\left|\boldsymbol{R}-\frac{m_f}{m_P}\boldsymbol{r}\right|}-\frac{1}{R}\right)dZ, \tag{22}$$

where $\omega = (E-E_0)/\hbar$, with E the c-f relative energy after dissociation. Because no adiabatic approximation is made in perturbation theory, this term does not diverge. When the adiabatic approximation is applied to Eq. (22), i.e., when ω is set to 0, one recovers exactly the Coulomb eikonal phase (16). This suggests that without adiabatic approximation the first-order term in Eq. (20) would be $i\chi^{\mathrm{FO}}$ (22). Furthermore, a simple analytic expression is available for each of the Coulomb multipoles in the far-field approximation, i.e., for $m_f r/m_P < R$ [39]. The idea of the correction is therefore to replace the exponential of the eikonal phase according to

$$e^{i\chi} \to e^{i\chi^N}\left(e^{i\chi^C} - i\chi^C + i\chi^{\mathrm{FO}}\right)e^{i\chi^C_{PT}}. \tag{23}$$

With this Coulomb correction, the breakup of halo nuclei can be described within the eikonal model taking on (nearly) the same footing both Coulomb and nuclear interactions at all orders. This correction can also be seen as an inexpensive way to introduce higher-order effects and nuclear interactions in the first-order perturbation theory.

In this work, we analyze the validity of this CCE model by comparing results obtained with the correction (23) to results of the DEA. The latter is chosen as reference calculation, because it does not make use of the adiabatic approximation that leads to the divergence in the eikonal description of breakup. It is also in good agreement with experiments [29,30]. Calculations performed in the usual eikonal model, and at the first-order of the perturbation theory will also be presented to emphasize the effects of the correction. We focus on the case of ^{11}Be breakup. In that case, only the dipole term of the Coulomb interaction is significant [40]. We thus restrict the correction to that multipole. The perturbative correction then reads [35]

$$\chi^{\mathrm{FO}}(\boldsymbol{b},\boldsymbol{r}) = -\eta\frac{m_f}{m_P}\frac{2\omega}{v}\left[K_1\left(\frac{\omega b}{v}\right)\hat{\boldsymbol{b}}\cdot\boldsymbol{s} + iK_0\left(\frac{\omega b}{v}\right)z\right], \tag{24}$$

where K_n are modified Bessel functions [37]. Of course, in other cases, like in ^{8}B Coulomb breakup, the quadrupole term may no longer be negligible [14,30], it should then be included in the correction.

C. Breakup cross sections

To evaluate breakup cross sections within the CCE we proceed as explained in Ref. [29], replacing the DEA breakup amplitude by

$$S^{(m_0)}_{kljm}(b) = e^{i(\sigma_l+\delta_{lj}-l\pi/2+\chi^C_{PT})}\langle\phi_{ljm}(E)|e^{i\chi^N} \times\left(e^{i\chi^C} - i\chi^C + i\chi^{\mathrm{FO}}\right)|\phi_{l_0 j_0 m_0}(E_0)\rangle, \tag{25}$$

where σ_l is the Coulomb phase shift [37]. The breakup amplitudes for the usual eikonal model are obtained in the same way but without the correction.

In the following, we consider two breakup observables. The first is the breakup cross section as a function of the c-f relative energy E after dissociation {see Eq. (52) of Ref. [29]}

$$\frac{d\sigma_{\mathrm{bu}}}{dE} = \frac{4\mu_{cf}}{\hbar^2 k}\frac{1}{2j_0+1}\sum_{m_0}\sum_{ljm}\int_0^\infty bdb\left|S^{(m_0)}_{kljm}(b)\right|^2. \tag{26}$$

This energy distribution is the observable usually measured in breakup experiments [11,12]. It corresponds to an incoherent sum of breakup probabilities computed at each b

$$\frac{dP_{\mathrm{bu}}}{dE}(E,b) = \frac{4\mu_{cf}}{\hbar^2 k}\frac{1}{2j_0+1}\sum_{m_0}\sum_{ljm}\left|S^{(m_0)}_{kljm}(b)\right|^2. \tag{27}$$

The second breakup observable is the parallel-momentum distribution {see Eq. (53) of Ref. [29]}

$$\frac{d\sigma_{\rm bu}}{dk_\parallel} = \frac{8\pi}{2j_0+1}\sum_{m_0}\int_0^\infty bdb\int_{|k_\parallel|}^\infty \frac{dk}{k}\sum_{\nu m} \times \left|\sum_{lj}(lIm-\nu\nu|jm)Y_l^{m-\nu}(\theta_k,0)S_{kljm}^{(m_0)}(b)\right|^2, \quad (28)$$

where $\theta_k = \arccos(k/k_\parallel)$ is the colatitude of the c-f relative wave vector $\boldsymbol{k}$ after breakup. Contrary to the energy distribution, the parallel-momentum distribution corresponds to a coherent sum of breakup amplitudes. This observable is therefore sensitive to interferences between different partial waves. Consequently, it constitutes a particularly severe test for reaction models.

III. NUMERICAL ASPECTS

For these calculations, we use the same description of ^{11}Be as in Ref. [41]. The halo nucleus is seen as a neutron loosely bound to a ^{10}Be core in its 0^+ ground state. The ^{10}Be-n interaction is simulated by a Woods-Saxon potential plus a spin-orbit coupling term (see Sec. IVA of Ref. [41]). The potential is adjusted to reproduce the first three levels of the ^{11}Be spectrum. The $\frac{1}{2}^+$ ground state is seen as a $1s1/2$ state, whereas the $\frac{1}{2}^-$ excited state is described by a $0p1/2$ state. This well-known shell inversion is obtained by considering a parity-dependent depth of the central term of the potential. The $\frac{5}{2}^+$ resonance at 1.274 MeV above the one-neutron separation threshold is simulated in the $d5/2$ partial wave.

The interaction between the projectile components and the target are simulated by optical potentials chosen in the literature. In our calculations, we use the same potentials as in Refs. [27,41]. As suggested in Ref. [42], the ^{10}Be-Pb potential is scaled from a parametrisation of Bonin *et al.* [43] that describes elastic scattering of 699 MeV α particles on lead {potential (1) in Table III of Ref. [27]}. For the ^{10}Be-C interaction, we use the potential developed by Al-Khalili, Tostevin, and Brooke, which reproduces the elastic scattering of ^{10}Be on C at 59.4 MeV/nucleon [44] (potential ATB in Table III of Ref. [41]). In both cases, we neglect the possible energy dependence of the potential. We model the neutron-target interaction with the Becchetti and Greenlees parametrization [45].

To evaluate the breakup amplitude (25) within the CCE or the usual eikonal model, we need to compute the eikonal phase (15). The nuclear part is evaluated numerically, whereas the Coulomb part is obtained from its analytic expression (17). The numerical integral over Z is performed on a uniform mesh from $Z_{\rm min} = -20$ fm to $Z_{\rm max} = 20$ fm with step $\Delta Z = 1$ fm. The corrected phase (23) is then numerically expanded into multipoles of rank λ. We use a Gauss quadrature on the unit sphere similar to the one considered to solve the time-dependent Schrödinger equation in Ref. [27]. The number of points along the colatitude is set to $N_\theta = 12$, and the number of points along the azimuthal angle is $N_\varphi = 30$. Unless otherwise stated, we perform all calculations with multipoles up to $\lambda_{\rm max} = 12$.

The eigenfunctions of the projectile Hamiltonian H_0 (1) are computed numerically with the Numerov method using 1000 radial points equally spaced from $r = 0$ up to $r = 100$ fm. The same grid is used to compute the radial integral in Eq. (25). For Coulomb (nuclear) breakup, the integrals over b appearing in Eqs. (26) and (28) are performed numerically from $b = 0$ up to $b = 300\,(100)$ fm with a step $\Delta b = 0.5\,(0.25)$ fm.

The DEA Schrödinger equation (10) is solved using the numerical technique detailed in Ref. [27]. In this technique, the projectile internal wave function is expanded on a three-dimensional spherical mesh. The size of the mesh required for the calculation varies with the projectile-target interaction. For Coulomb- (nuclear) dominated reactions, the angular grid contains up to $N_\theta = 8$ (12) points along the colatitude θ, and $N_\varphi = 15$ (23) points along the azimuthal angle φ. This corresponds to an angular basis that includes all possible spherical harmonics up to $l = 7$ (11). The radial variable r is discretized on a quasiuniform mesh that contains $N_r = 800$ (600) points and extends up to $r_{N_r} = 800$ (600) fm. The time propagation is performed with a second-order approximation of the evolution operator. It is started at $t_{\rm in} = -20\,(10)\,\hbar/$MeV with the projectile in its initial bound state and is stopped at $t_{\rm out} = 20\,(10)\,\hbar/$MeV ($t = 0$ corresponds to the time of closest approach). The time step is set to $\Delta t = 0.02\,\hbar/$MeV in both Coulomb and nuclear cases.

The evolution calculations are performed for different values of b. These values range from 0 up to 300 (100) fm with a step Δb varying from 0.5 (0.25) fm to 5.0 (2.0) fm, depending on b. The integrals over b are performed numerically.

IV. BREAKUP OF ^{11}Be ON Pb AT 69 MeV/NUCLEON

We first consider the breakup of ^{11}Be on lead at 69 MeV/nucleon, which corresponds to the experiment of Fukuda *et al.* at RIKEN [12]. These data are fairly well reproduced by the DEA [29], that we use as reference calculation. Because we focus on the comparison of models, we do not display Fukuda's measurements. A comparison with experiment would indeed require a convolution of our results, which would hinder the comparison between theories.

In Fig. 2, we compare the breakup probability (27) obtained with the DEA (full lines), the CCE (dotted lines), the usual eikonal model (Eik., dashed lines), and the first-order perturbation theory (FO, dash-dotted line). They are depicted as a function of the transverse coordinate b for three ^{10}Be-n relative energies: $E = 0.5$ MeV, 1.274 MeV (i.e., the $\frac{5}{2}^+$ resonance energy), and 3.0 MeV. The upper part of Fig. 2 displays the values at small b, whereas the lower part, in a semilogarithmic scale, focuses on the asymptotic region.

Over the whole range in b, the CCE results are close to the DEA ones, and this at all energies. This good agreement suggests the Coulomb correction to be valid for simulating the breakup of loosely bound nuclei on heavy targets. In particular, the CCE is superimposed to the DEA results in

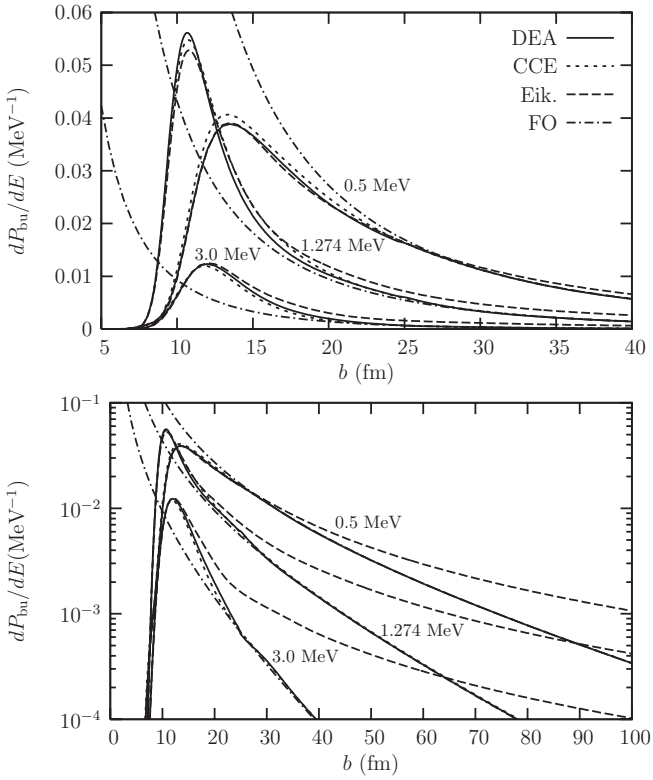

FIG. 2. Breakup probabilities as a function of transverse coordinate b for ^{11}Be impinging on ^{208}Pb at 69 MeV/nucleon. Three energies E are shown: 0.5, 1.274, and 3.0 MeV. The results are obtained within DEA (full lines), CCE (dotted lines), usual eikonal approximation (dashed lines), and first-order perturbation theory (dash-dotted lines). The upper part displays the values at small b, whereas the lower part focuses on the asymptotic region.

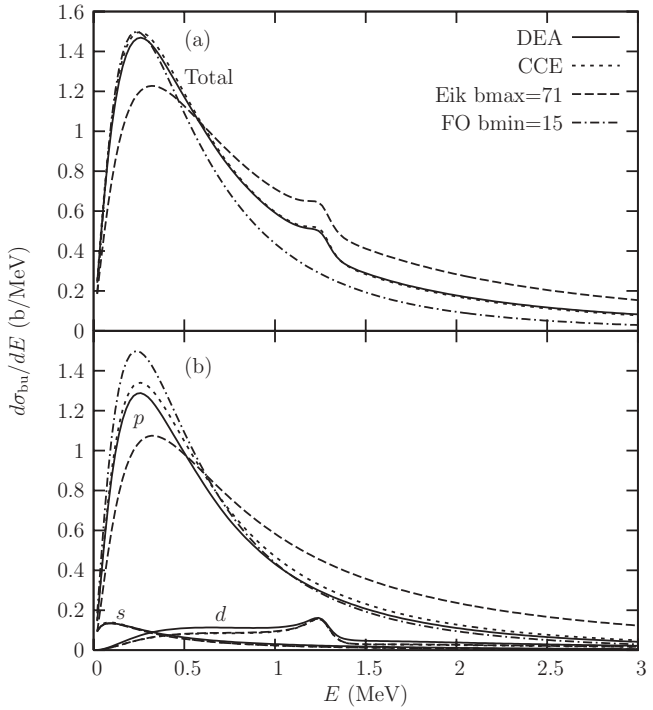

FIG. 3. (a) Breakup cross sections for ^{11}Be impinging on ^{208}Pb at 69 MeV/nucleon as a function of the ^{10}Be-n relative energy E. The results are obtained within the DEA, the CCE, the usual eikonal approximation with upper cutoff $b_{max} = 71$ fm, and the first-order perturbation theory with lower cutoff $b_{min} = 15$ fm. (b) Contributions of the s, p, and d partial waves.

the asymptotic region. Obviously, the first-order perturbation theory efficiently corrects the erroneous $1/b$ asymptotic behavior of the usual eikonal model.

At small b, the agreement between the CCE and DEA seems slightly less good. In particular, at small energy, the corrected eikonal model overestimates the reference calculation. This is due to the far-field approximation used in the first-order perturbation correction. This approximation provides a convenient analytical expression (24) of the phase χ^{FO}. However, it is incorrect at small b: it diverges at $b = 0$. Nevertheless, in spite of that divergence, the CCE remains close to the DEA. This illustrates that the CCE can also be seen as a way to include nuclear interactions within the first-order perturbation theory and correct its ill-behavior at small b.

The breakup cross section (26) computed with the four approximations is displayed in Fig. 3(a) as a function of the ^{10}Be-n relative energy E after dissociation. Contributions of the s, p, and d partial waves are shown separately in Fig. 3(b). The small bump at about 1.25 MeV is due to the resonance in the $d5/2$ partial wave. The CCE cross section (dotted line) is nearly superimposed on the DEA one (full line). Only at low energy is the CCE slightly larger than the reference calculation. As mentioned earlier this effect is due to the use of the far-field approximation to derive the perturbative correction χ^{FO}.

Interestingly, the agreement between CCE and DEA is better for the total cross section than for each partial-wave contribution: The CCE p contribution is larger than the DEA one, whereas the CCE s and d contributions are smaller than the DEA ones. We interpret this as a lack of couplings in the continuum in the CCE. In the DEA, these couplings depopulate the p waves toward the s and d ones without modifying the total cross section [40]. The differences between CCE and DEA partial-wave contributions suggest that this mechanism is hindered in the former.

The wrong asymptotic behavior of the Coulomb eikonal phase (17) leads to a divergence in the calculation of the breakup cross sections. To evaluate the energy distribution within the usual eikonal model one needs to resort to a cutoff at large b. The cutoff proposed in Ref. [38] [see also Eq. (21)] gives here $b_{max} = 71$ fm. The corresponding cross section is displayed in Fig. 3(a) with a dashed line. Its energy dependence is strongly different from that of the reference calculation: it is too small at low energy and too large at high energy. The p contribution, which includes the diverging term of the Coulomb eikonal phase (17), is responsible for that ill behavior. Contrarily, the s and d contributions are superimposed on those of the CCE. The use of the Coulomb correction therefore significantly improves the eikonal model when considering collisions with heavy targets.

The cross section obtained within the first-order perturbation theory is shown in dot-dashed line. The nuclear

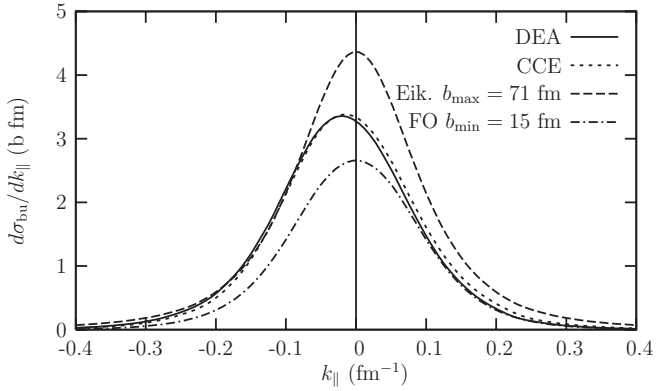

FIG. 4. Breakup cross sections for ^{11}Be impinging on ^{208}Pb at 69 MeV/nucleon as a function of the ^{10}Be-n relative parallel momentum $k_{\parallel}$. The figure displays the results obtained within the DEA, the CCE, the usual eikonal approximation with an upper cutoff $b_{\max} =$ 71 fm, and the first-order perturbation theory with a lower cutoff $b_{\min} = 15$ fm.

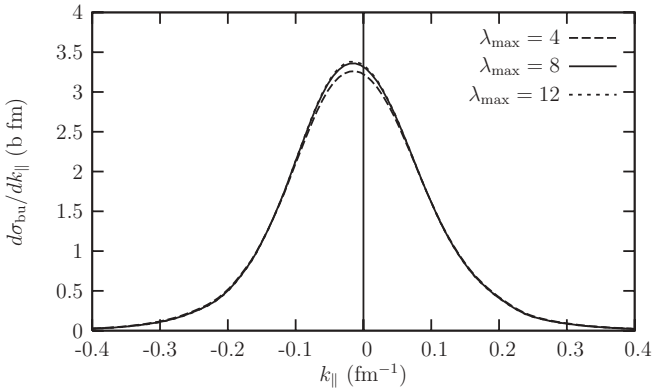

FIG. 5. Convergence of the multipole expansion in $\lambda_{\max}$ of the CCE illustrated on the parallel-momentum distribution computed for ^{11}Be impinging on ^{208}Pb at 69 MeV/nucleon.

interactions between the projectile and the target are described by a mere cutoff at $b_{\min} = 15$ fm. This value has been chosen to fit the DEA energy distribution in the region of the maximum. Here again, the shape of the cross section is very different from that of the reference calculation. However, contrary to the usual eikonal model, it decreases too quickly with the energy. Moreover, because only the dipole term of the Coulomb interaction is considered, only the p wave is reached from the s ground state, whereas s and d waves are significantly populated through nuclear interactions and higher-order effects. Note that a smaller cutoff $b_{\min}$, in better agreement with the usual choice that corresponds to the sum of the projectile and target radii, does not improve the agreement.

We now consider the parallel-momentum distribution [see Eq. (28)]. This breakup observable is more sensitive to interferences and therefore constitutes a more severe test than the energy distribution. The parallel-momentum distribution computed within the four models is displayed in Fig. 4.

As in the previous cases, the CCE is in excellent agreement with the DEA in both magnitude and shape. We simply note that the former is slightly less asymmetric than the latter, which is probably a signature of the lack of couplings in the continuum mentioned earlier. On the contrary, both the usual eikonal model and the first-order perturbation theory lead to rather poor estimates of the momentum distribution. First, they lead to an erroneous magnitude of the cross section. The usual eikonal model gives too large a parallel-momentum distribution. This is related to the too-slow decrease obtained for the energy distribution. On the contrary, the first-order perturbation gives too low a cross section; a defect due to the quick decrease in the energy distribution. Lowering the cutoff $b_{\min}$ to cure this problem would then lead to too large an energy distribution in the peak region. Second, none of these models exhibits the asymmetry observed in the DEA. This absence of asymmetry in parallel-momentum distributions of the breakup of loosely bound projectiles is a well-known problem of the eikonal model [46]. It is fortunate that the Coulomb correction, combining two approximations that lead to perfectly symmetric momentum distributions, restores the asymmetry observed experimentally and in dynamical calculations.

Figure 5 illustrates the convergence of the CCE with regard to the number of multipoles considered in the breakup computation. The parallel-momentum distributions obtained with maximum multipolarities $\lambda_{\max} = 4$, 8, and 12 are displayed. Although all three calculations are close to one another, $\lambda_{\max} = 4$ has not yet converged: there remains some 4% difference with the other two at the maximum. On the contrary, the difference between $\lambda_{\max} = 8$ and 12 is insignificant (about 0.5%). This shows the necessity to include a large number of partial waves in dynamical calculations. Note that other breakup observables converge with a lower number of multipoles. In particular, the energy distribution requires only $\lambda_{\max} = 4$ to reach satisfactory convergence.

These results confirm the ability of the Coulomb correction to reliably reproduce breakup observables for collisions of loosely bound projectiles on heavy targets. It reproduces dynamical calculations with an accuracy that is unreachable within the usual eikonal model or the first-order perturbation theory on which it is based.

V. BREAKUP OF ^{11}Be ON C AT 67 MeV/NUCLEON

To complete this analysis of the Coulomb correction, we investigate its effect in nuclear induced breakup. The usual eikonal description of such reactions is known to give excellent results [17,29]. The Coulomb interaction between the projectile and the target plays then a minor role and we expect the correction (23) to have much less influence than in the Coulomb breakup case.

For this analysis, we consider the breakup of ^{11}Be on a carbon target at 67 MeV/nucleon, which corresponds to the experiment of Fukuda *et al.* [12]. The DEA is in excellent agreement with Fukuda's data [29], and therefore constitutes our reference calculation. For the same reasons as in the previous section, we do not compare directly our calculations with experiment.

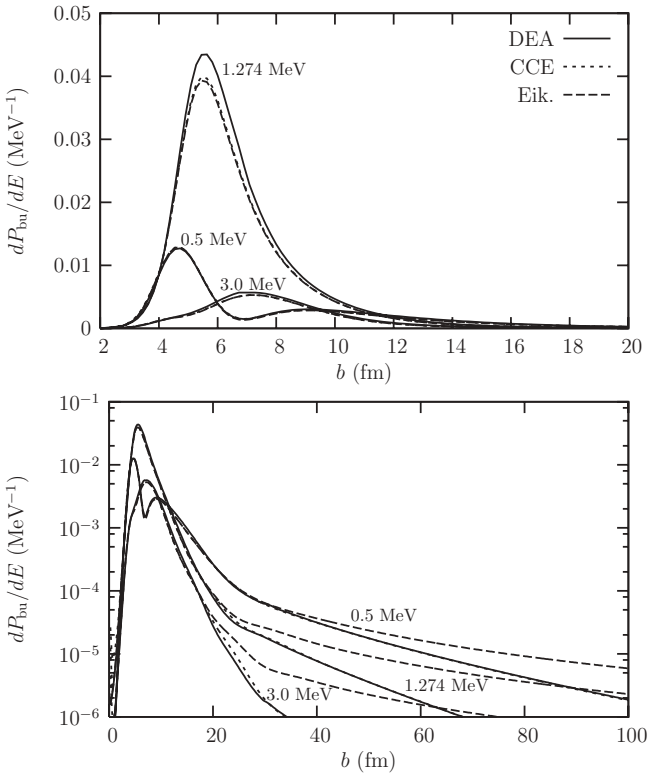

FIG. 6. Breakup probabilities as a function of transverse coordinate b for ^{11}Be impinging on ^{12}C at 67 MeV/nucleon. Three energies E are shown: 0.5, 1.274, and 3.0 MeV. The results are obtained within the DEA (full lines), CCE (dotted lines), and usual eikonal (dashed lines) models. The upper part displays the values at small b, whereas the lower part emphasizes the behavior in the asymptotic region.

Figure 6 displays the breakup probability (27) obtained at three energies $E = 0.5, 1.274$, and 3.0 MeV within the DEA (full lines), the CCE (dotted lines), and the usual eikonal model (dashed lines). Because this reaction is nuclear dominated, we no longer display the result of the first-order perturbation theory. The upper part of Fig. 6 displays the breakup probability at small b, whereas the lower part emphasizes the asymptotic behavior of P_{bu} in a semilogarithmic plot.

In this case, all three reaction models lead to similar results. This confirms the validity of the adiabatic approximation in the eikonal description of nuclear-dominated reactions. The difference between the DEA and the other two models is indeed rather small. Only at $E = 1.274$ MeV, the energy of the $\frac{5}{2}^+$ resonance, does it become significant (up to 10% difference in the vicinity of the peak at $b \sim 6$ fm). This larger difference suggests stronger dynamical effects at the resonance. This is not very surprising because the presence of that resonance strongly increases the breakup process [41].

Up to $b = 20$ fm, the usual eikonal model and the CCE remain very close to one another, confirming the small role played by the Coulomb interaction in the dissociation. At larger b, where only Coulomb is significant, we observe the $1/b$ behavior of the usual eikonal model. This ill behavior is corrected using the CCE, whose breakup probabilities are nearly superimposed on the DEA ones in the asymptotic region. However, because this correction affects breakup probabilities at two or three orders of magnitude below the maximum, we do not expect it to significantly influence breakup observables.

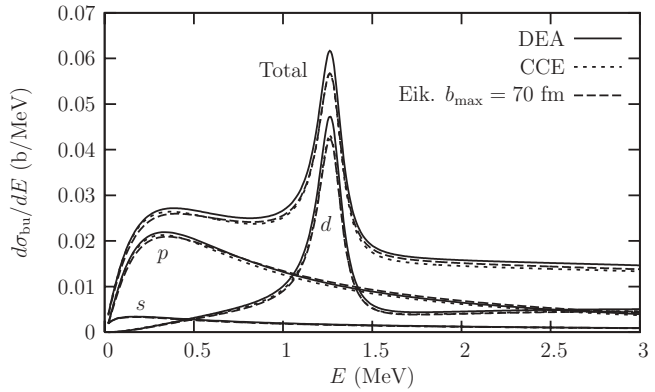

FIG. 7. Breakup cross sections for ^{11}Be impinging on ^{12}C at 67 MeV/nucleon as a function of the ^{10}Be-n relative energy E. Results are obtained within the DEA, the CCE, and the usual eikonal model with an upper cutoff $b_{max} = 70$ fm. Contributions of the s, p, and d partial waves are shown as well.

The breakup cross sections computed within the three models are plotted as functions of the energy E in Fig. 7. The contributions to the total cross section of the partial waves s, p, and d are shown as well. The large peak at about 1.25 MeV is the signature of the significant enhancement of the breakup process by the $d5/2$ resonance. As suggested by the previous result, all three models lead to very similar cross sections. This similarity is also observed in the partial-wave contributions. The couplings in the continuum that depopulate one partial wave toward others, as observed in Coulomb breakup (see Fig. 3 and Ref. [40]), are thus much smaller in nuclear-induced breakup.

As in Fig. 6, the difference between the DEA and the other two models is rather small. The DEA is about 6% in average larger than the eikonal model. Note that this difference reaches 8% at the resonance energy, which is consistent with the difference observed in Fig. 6(a). The usual eikonal and the CCE lie even closer to one another. The relative difference between them in the total cross section does not exceed 3%. Even in the p partial wave, where the Coulomb correction is performed, no significant difference is observed. This confirms that the correction of the eikonal model is not necessary for nuclear-dominated reactions due to the small role played by the Coulomb interaction. The cutoff in b proposed in Ref. [38] is therefore sufficient.

The parallel-momentum distributions obtained with the three models are displayed in Fig. 8. As already mentioned, this observable is a more severe test for reaction models than the energy distribution. We observe significant differences between the DEA and the other two models. As in the case of Coulomb breakup, the DEA leads to an asymmetric parallel-momentum distribution: The DEA distribution is shifted toward negative $k_\parallel$ and presents a more developed tail on the negative $k_\parallel$ side, as observed in Ref. [46].

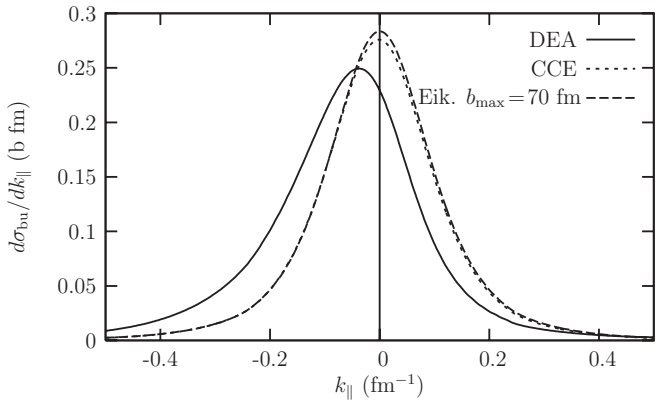

FIG. 8. Breakup cross sections for ^{11}Be impinging on ^{12}C at 67 MeV/nucleon as a function of the ^{10}Be-n relative parallel momentum $k_{\parallel}$. Results are obtained within the DEA, the CCE, and the usual eikonal approximation with an upper cutoff $b_{max} = 70$ fm.

As for the previous observable, the CCE and usual eikonal models lead to very similar parallel-momentum distributions. These distributions are symmetric. As mentioned earlier, this symmetry is due to the lack of dynamical effects in the eikonal description of reactions. Contrary to the Coulomb case, the correction (23) is not able to restore this asymmetry. It indicates that these dynamical effects result from the nuclear interactions between the projectile and the target.

The convergence of the CCE model with the number of multipoles is illustrated in Fig. 9 for the parallel-momentum distribution. The CCE distributions computed with $\lambda_{max} =$ 4–12 are displayed. The convergence is much slower than for Coulomb-dominated breakup (see Fig. 5). The relative difference between $\lambda_{max} = 10$ and $\lambda_{max} = 12$ is indeed about 3% at the maximum. This is due to the rapid variation of the nuclear potential with the projectile-target coordinates. It confirms the need of a larger number of partial waves in the dynamical calculation of nuclear-dominated dissociation. Note that the convergence is faster for the energy distribution. For that observable, an acceptable convergence is reached at $\lambda_{max} = 6$.

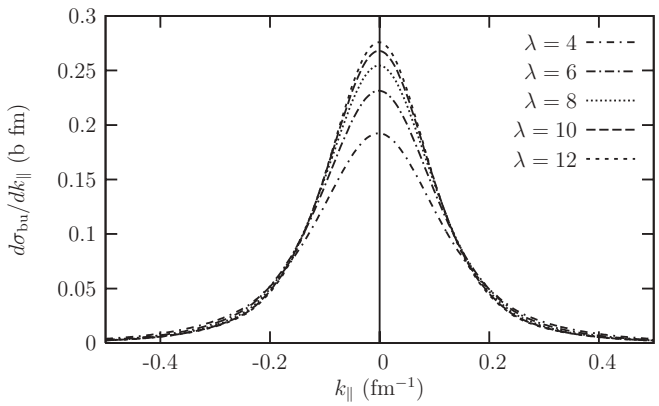

FIG. 9. Convergence in λ_{max} of the CCE illustrated on the parallel-momentum distribution for the breakup of ^{11}Be on ^{12}C at 67 MeV/nucleon.

VI. CONCLUSION

The eikonal description of reactions is a useful tool to simulate breakup and stripping reactions on light targets at intermediate and high energies [16,17,29]. This model is interesting because of its relative simplicity in implementation and interpretation with respect to other elaborate models, like CDCC or DEA. Unfortunately, it suffers from a divergence problem associated with the treatment of the Coulomb interaction between the projectile and the target. This divergence is due to the incompatibility of the adiabatic, or sudden, approximation that is made in the usual eikonal model and the infinite range of the Coulomb interaction. One way to cure this problem is not to make this adiabatic approximation. This leads to the DEA [28,29]. However, like other elaborate models, the DEA is computationally expensive. Another way to solve this problem is to substitute the diverging Coulomb phase at the first order of the eikonal model by the corresponding first order of the perturbation theory [34,35].

In this work, we study the validity of this Coulomb correction by comparing it to the DEA, which does not present the divergence problem of the usual eikonal model. The chosen test cases are the dissociation of ^{11}Be on Pb and C at about 70 MeV/nucleon. These correspond to RIKEN experiments [11,12] that are well reproduced by the DEA [29].

In the case of the Coulomb breakup, the CCE gives results in excellent agreement with the DEA. The combination of the eikonal model with the first-order perturbation theory indeed solves the divergence problem due to the Coulomb interaction. Moreover, it correctly takes into account the nuclear interaction between the projectile and target. The breakup observables (energy and parallel-momentum distributions) obtained within the DEA are accurately reproduced using the CCE. This agreement is obtained while both CCE ingredients—usual eikonal and first-order perturbation—fail to describe the reaction. First, they both require a rather arbitrary upper or lower cutoff in b so as not to diverge. Second, they do not reproduce the shape of the breakup cross sections. In particular the CCE gives an asymmetric parallel-momentum distribution, in agreement with the dynamical calculation. Contrarily, both the usual eikonal and the perturbative models lead to perfectly symmetric distributions. This suggests that CCE restores dynamical effects that are missing in its ingredients.

The Coulomb correction has much less effect on the nuclear-dominated breakup. This was expected because of the much smaller influence of the Coulomb interaction in reactions involving light targets. This result indicates that in this case the correction is not essential. It also implies that the CCE suffers the same lack of dynamical effects as the usual eikonal model in nuclear dominated reactions.

The CCE successfully combines the positive aspects of both the eikonal model and the first-order perturbation theory. It allows describing accurately the nuclear interaction while correctly reproducing Coulomb-induced effects. Moreover, the CCE restores some of the dynamical effects, which are totally absent in other simple models. It therefore provides a reliable description of the breakup of loosely bound projectiles at intermediate and high energies. Its simplicity in use and interpretation suggests it as a competitive alternative to more

elaborate models to describe the breakup of Borromean nuclei.

ACKNOWLEDGMENTS

This work has been done in the framework of the agreement between the Japan Society for the Promotion of Science (JSPS) and the Fund for Scientific Research of Belgium (F. R. S.-FNRS). Y. S. acknowledges the support of the Grant for the Promotion of Niigata University Research Projects (2005–2007). P. C. acknowledges travel support of the Fonds de la Recherche Scientifique Collective (FRSC) and the support of the F. R. S.-FNRS. This text presents research results of the Belgian program P6/23 on interuniversity attraction poles initiated by the Belgian-state Federal Services for Scientific, Technical and Cultural Affairs (FSTC).

[1] P. G. Hansen, A. S. Jensen, and B. Jonson, Annu. Rev. Nucl. Part. Sci. **45**, 591 (1995).
[2] I. Tanihata, J. Phys. G **22**, 157 (1996).
[3] B. Jonson, Phys. Rep. **389**, 1 (2004).
[4] P. G. Hansen and B. Jonson, Europhys. Lett. **4**, 409 (1987).
[5] M. V. Zhukov, B. V. Danilin, D. V. Fedorov, J. M. Bang, I. J. Thompson, and J. S. Vaagen, Phys. Rep. **231**, 151 (1993).
[6] I. Tanihata, H. Hamagaki, O. Hashimoto, S. Nagamiya, Y. Shida, N. Yoshikawa, O. Yamakawa, K. Sugimoto, T. Kobayashi, D. E. Greiner *et al*., Phys. Lett. **B160**, 380 (1985).
[7] I. J. Thompson and Y. Suzuki, Nucl. Phys. **A693**, 424 (2001).
[8] J. Al-Khalili and F. M. Nunes, J. Phys. G **29**, R89 (2003).
[9] G. Baur, K. Hencken, and D. Trautmann, Prog. Part. Nucl. Phys. **51**, 487 (2003).
[10] T. Kobayashi, S. Shimoura, I. Tanihata, K. Katori, K. Matsuta, T. Minamisono, K. Sugimoto, W. Müller, D. L. Olson, T. L. M. Symon *et al*., Phys. Lett. **B232**, 51 (1989).
[11] T. Nakamura, S. Shimoura, T. Kobayashi, T. Teranishi, K. Abe, N. Aoi, Y. Doki, M. Fujimaki, N. Inabe, N. Iwasa *et al*., Phys. Lett. **B331**, 296 (1994).
[12] N. Fukuda, T. Nakamura, N. Aoi, N. Imai, M. Ishihara, T. Kobayashi, H. Iwasaki, T. Kubo, A. Mengoni, M. Notani *et al*., Phys. Rev. C **70**, 054606 (2004).
[13] S. Typel and G. Baur, Phys. Rev. C **50**, 2104 (1994).
[14] H. Esbensen and G. F. Bertsch, Nucl. Phys. **A600**, 37 (1996).
[15] J. A. Tostevin, S. Rugmai, and R. C. Johnson, Phys. Rev. C **57**, 3225 (1998).
[16] R. J. Glauber, in *Lectures in Theoretical Physics*, edited by W. E. Brittin and L. G. Dunham (Interscience, New York, 1959), Vol. 1, p. 315.
[17] Y. Suzuki, R. G. Lovas, K. Yabana, and K. Varga, *Structure and Reactions of Light Exotic Nuclei* (Taylor & Francis, London, 2003).
[18] C. A. Bertulani and P. Danielewicz, *Introduction to Nuclear Reactions* (Institute of Physics Publishing, Bristol, 2004).
[19] M. Kamimura, M. Yahiro, Y. Iseri, H. Kameyama, Y. Sakuragi, and M. Kawai, Prog. Theor. Phys. Suppl. **89**, 1 (1986).
[20] N. Austern, Y. Iseri, M. Kamimura, M. Kawai, G. Rawitscher, and M. Yahiro, Phys. Rep. **154**, 125 (1987).
[21] J. A. Tostevin, F. M. Nunes, and I. J. Thompson, Phys. Rev. C **63**, 024617 (2001).
[22] T. Kido, K. Yabana, and Y. Suzuki, Phys. Rev. C **50**, R1276 (1994).
[23] T. Kido, K. Yabana, and Y. Suzuki, Phys. Rev. C **53**, 2296 (1996).
[24] H. Esbensen, G. F. Bertsch, and C. A. Bertulani, Nucl. Phys. **A581**, 107 (1995).
[25] S. Typel and H. H. Wolter, Z. Naturforsch. Teil A **54**, 63 (1999).
[26] V. S. Melezhik and D. Baye, Phys. Rev. C **59**, 3232 (1999).
[27] P. Capel, D. Baye, and V. S. Melezhik, Phys. Rev. C **68**, 014612 (2003).
[28] D. Baye, P. Capel, and G. Goldstein, Phys. Rev. Lett. **95**, 082502 (2005).
[29] G. Goldstein, D. Baye, and P. Capel, Phys. Rev. C **73**, 024602 (2006).
[30] G. Goldstein, P. Capel, and D. Baye, Phys. Rev. C **76**, 024608 (2007).
[31] N. C. Summers, F. M. Nunes, and I. J. Thompson, Phys. Rev. C **74**, 014606 (2006).
[32] T. Matsumoto, E. Hiyama, K. Ogata, Y. Iseri, M. Kamimura, S. Chiba, and M. Yahiro, Phys. Rev. C **70**, 061601(R) (2004).
[33] M. Rodríguez-Gallardo, J. M. Arias, J. Gómez-Camacho, R. C. Johnson, A. M. Moro, I. J. Thompson, and J. Tostevin, Phys. Rev. C **77**, 064609 (2008).
[34] J. Margueron, A. Bonaccorso, and D. M. Brink, Nucl. Phys. **A720**, 337 (2003).
[35] B. Abu-Ibrahim and Y. Suzuki, Prog. Theor. Phys. **112**, 1013 (2004); **114**, 901 (2005).
[36] K. Alder and A. Winther, *Electromagnetic Excitation* (North-Holland, Amsterdam, 1975).
[37] M. Abramowitz and I. A. Stegun, *Handbook of Mathematical Functions* (Dover, New York, 1970).
[38] B. Abu-Ibrahim and Y. Suzuki, Phys. Rev. C **62**, 034608 (2000).
[39] H. Esbensen and C. A. Bertulani, Phys. Rev. C **65**, 024605 (2002).
[40] P. Capel and D. Baye, Phys. Rev. C **71**, 044609 (2005).
[41] P. Capel, G. Goldstein, and D. Baye, Phys. Rev. C **70**, 064605 (2004).
[42] S. Typel and R. Shyam, Phys. Rev. C **64**, 024605 (2001).
[43] B. Bonin, N. Alamanos, B. Berthier, G. Bruge, H. Faraggi, J. C. Lugol, W. Mittig, L. Papineau, A. I. Yavin, J. Arvieux *et al*., Nucl. Phys. **A445**, 381 (1985).
[44] J. S. Al-Khalili, J. A. Tostevin, and J. M. Brooke, Phys. Rev. C **55**, R1018 (1997).
[45] F. D. Becchetti, Jr. and G. W. Greenlees, Phys. Rev. **182**, 1190 (1969).
[46] J. A. Tostevin, D. Bazin, B. A. Brown, T. Glasmacher, P. G. Hansen, V. Maddalena, A. Navin, and B. M. Sherrill, Phys. Rev. C **66**, 024607 (2002).